Supplementary material for

RNA methylation influences TDP43 binding and disease pathogenesis in models of amyotrophic lateral sclerosis and frontotemporal dementia

Michael McMillan[1,2#], Nicolas Gomez[1,2#], Caroline Hsieh[1,2], Michael Bekier[1], Xingli Li[1], Roberto Miguez[1], Elizabeth M.H. Tank[1] and Sami J. Barmada[1,2*]

[1]Department of Neurology, University of Michigan, Ann Arbor, MI, 48109, USA

[2]Graduate Program in Cell and Molecular Biology, University of Michigan, Ann Arbor, MI, 48109, USA

[#]Authors contributed equally

*To whom correspondence should be addressed:

Sami Barmada

University of Michigan

Department of Neurology

109 Zina Pitcher Place, 4019 BSRB

Ann Arbor, MI 48109

USA

Supplemental Fig. 1 HaloTag insertion in *TARDBP* locus does not affect TDP43 function

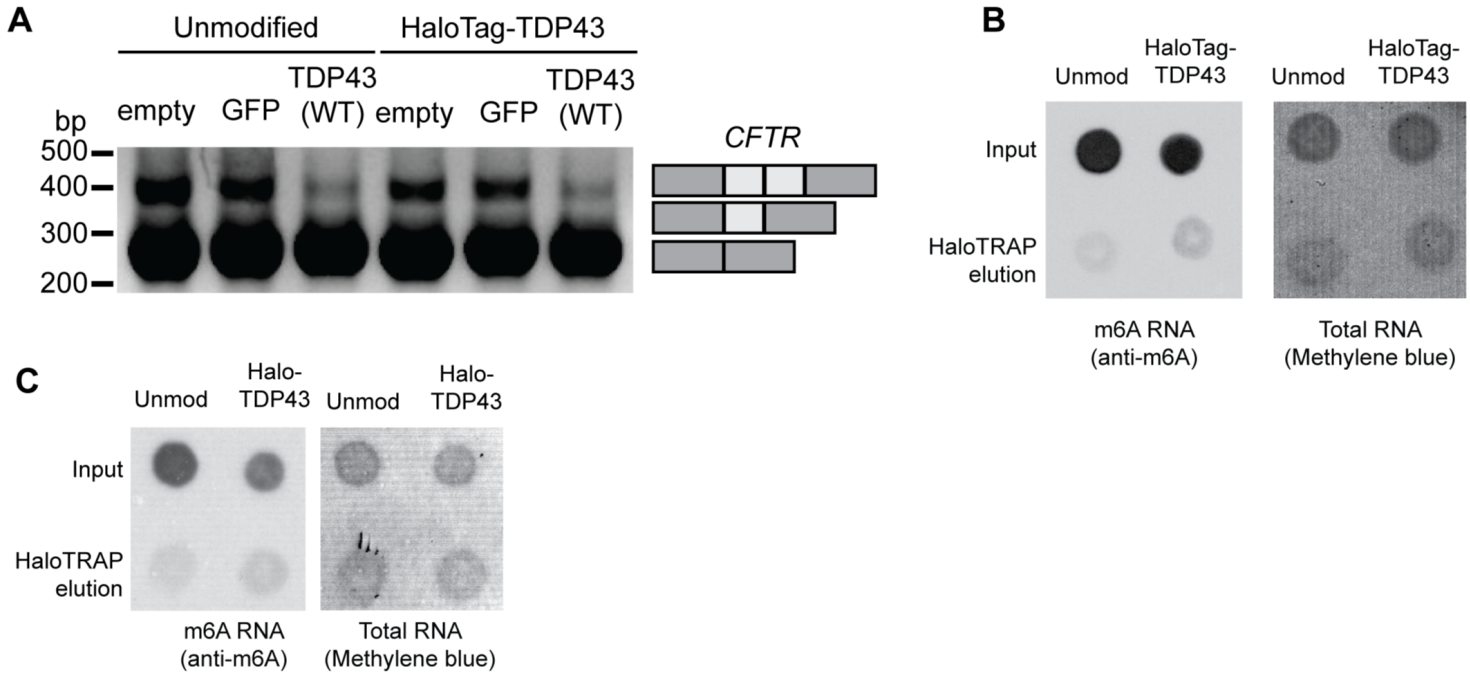

Supplemental figure 1: HaloTag insertion in *TARDBP* locus does not affect TDP43 function (related to Fig. 1). (**A**) *CFTR* minigene splicing assay[7,33,75] in which unmodified or HaloTag-TDP43 HEK293T cells were transfected with the CFTR minigene along with EGFP or TDP43-EGFP then analyzed by PCR amplification to measure functional TDP43. Correct TDP43 mediated splicing of the reporter results in exon 9 exclusion. (**B**) Additional dot blots for total RNA (detected by methylene blue) or m6A-modified RNA (detected by anti-m6A antibody) isolated by immunoaffinity purification of endogenous HaloTag-TDP43 or exogenous HaloTag using Synaptic Systems anti-m6a (#202003) or (**C**) Millipore Sigma anti-m6A (ABE572-I-100UG) antibodies.

Supplemental Fig. 2: Characterization of TDP43 binding sites, target gene ontology, and predicted protein networks

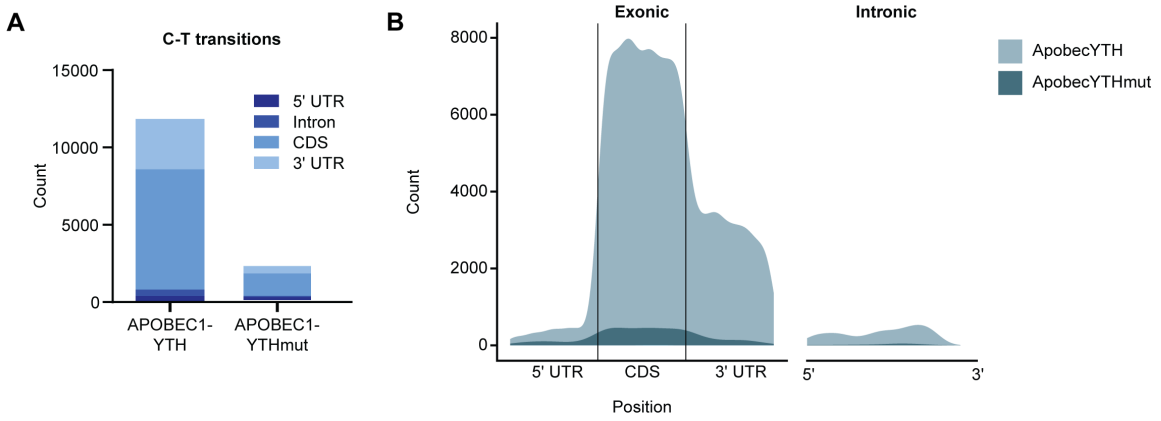

C **Biological process GO** for methylated Hallegger and DART-seq TDP43 targets (n=1699)

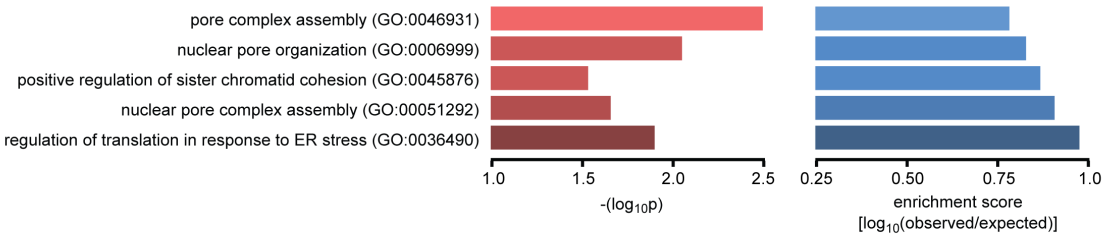

D **Protein-protein interaction (PPI) network** analysis for conserved TDP43 targets (n=1699)

cluster ID	#	examples	top KEGG pathway
1	24	CDK1, hnRNPC, HSPA4, HSPA5, XPOT	cell cycle
2	20	BCL2, CHEK1, CREB1, TAF15, TP53	apoptosis
3	20	EIF5, NOP58, RPL11, RPL17, RPS5	ribosome
4	18	CARM1, CREBBP, ATF4, ETS1, HSF1	long-term potentiation
5	17	DPHA2, LAMB1, CAPNS1, CDC42	VEGF signaling
6	17	NUP107, NUP153, NUP214, TNPO1	RNA transport
7	15	DCTN2, DCTN4, DYNC1H1, CAPZA1	vasopressin signaling
8	15	ARFGEF1, ADCY6, UBQLN1, CACNB2	GABAergic synapse
9	14	CDC6, DNA2, POLD2, POLE2, POLG	DNA replication
10	14	CNOT4, PTBP1, EIF4G1, CASP7	viral infection

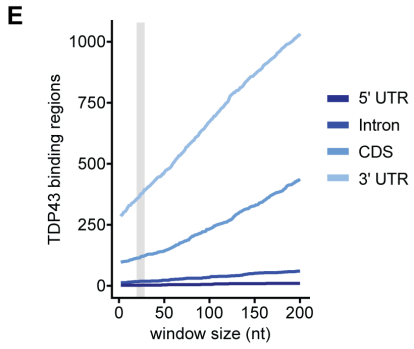

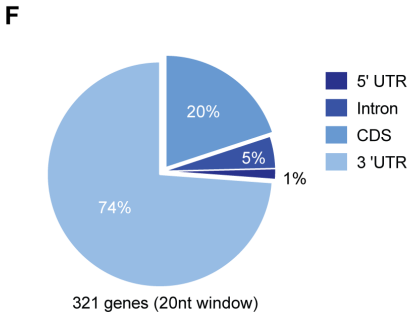

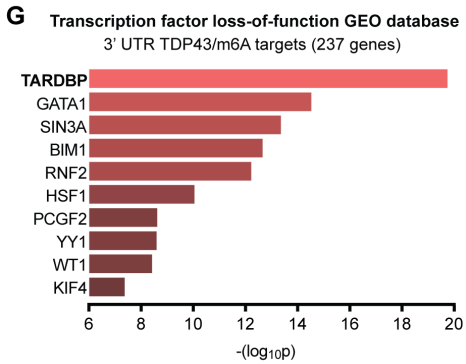

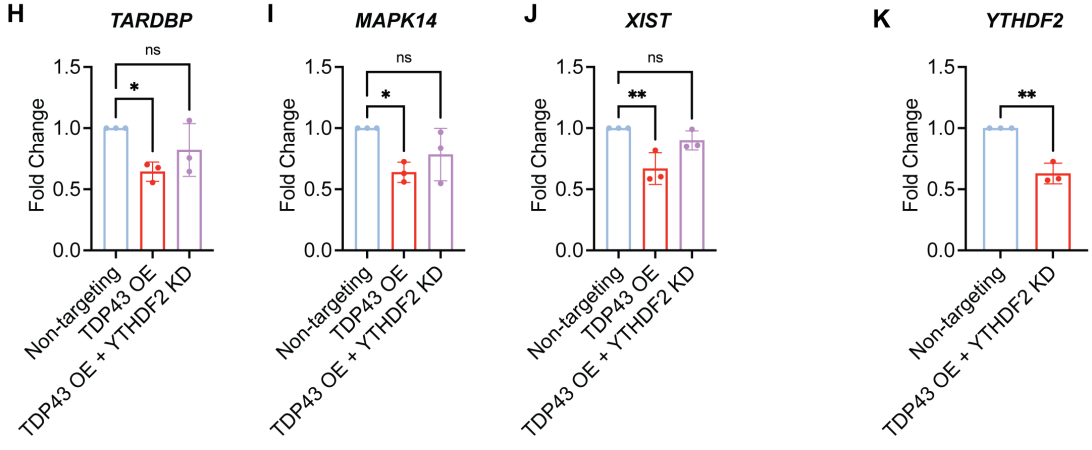

Supplemental figure 2: Characterization of TDP43 binding sites, target gene ontology, and predicted protein networks (related to Fig. 2). Absolute count (**A**) and relative distribution (**B**) of C-T transitions indicative of m6A modifications located within the coding sequence (CDS), 5' untranslated region (UTR), 3' UTR, and introns in cells expressing APOBEC1-YTH and APOBEC1-YTHmut. (**C**) Gene ontology for biological processes enriched in TDP43 substrate RNAs (n=1699) common to those identified in this study and Hallegger *et al.* 2021[1]. (**D**) Protein-protein interaction network analysis[2] for shared TDP43 targets shows enrichment of targets associated with ribosome, long term potentiation, VEGF signaling, and RNA transport. **(E)** Iterative topological mapping plot depicting the likelihood of finding a TDP43 binding site (as determined by CLIP-seq, Hallegger et al. 2021[1]) within the vicinity of a C-T transition (identified by DART-seq, this study), located at position 0. The magnitude and direction of the slopes for lines corresponding to each gene region indicates a positive relationship between TDP43 binding sites and m6A sites primarily within the 3' UTR, but also within the CDS. (**F**) In the subset of genes exhibiting a TDP43 binding site within 20nt of an m6A site (n=321; grey shading in **E**), this association was most often detected within the 3' UTR (237/321 genes, or 74%). (**G**) The 237 genes showing TDP43 binding sites and m6A sites within the 3'UTR were strongly enriched for genes whose expression is regulated by TDP43, as determined by comparison with the transcription factor loss-of-function GEO database. qRT-PCR analysis of (**H**) TARDBP, (**I**) MAPK14, and (**J**) XIST in HEK293 cells following TDP43 overexpression (OE) and/or YTHDF2 knockdown (KD). (**K**) Only partial KD of YTHDF2 was achieved by transfection with YTHDF2 shRNA. Data in (H)-(J) are shown as mean $\pm$ SD, collected from 3 biological replicates. In (F)-(H), **p<0.01, *p<0.05, one-way ANOVA with Dunnett's post test. In (K), **p<0.01, two-tailed t-test.

Supplemental Fig. 3: m6A modifications alter TDP43 binding capabilities

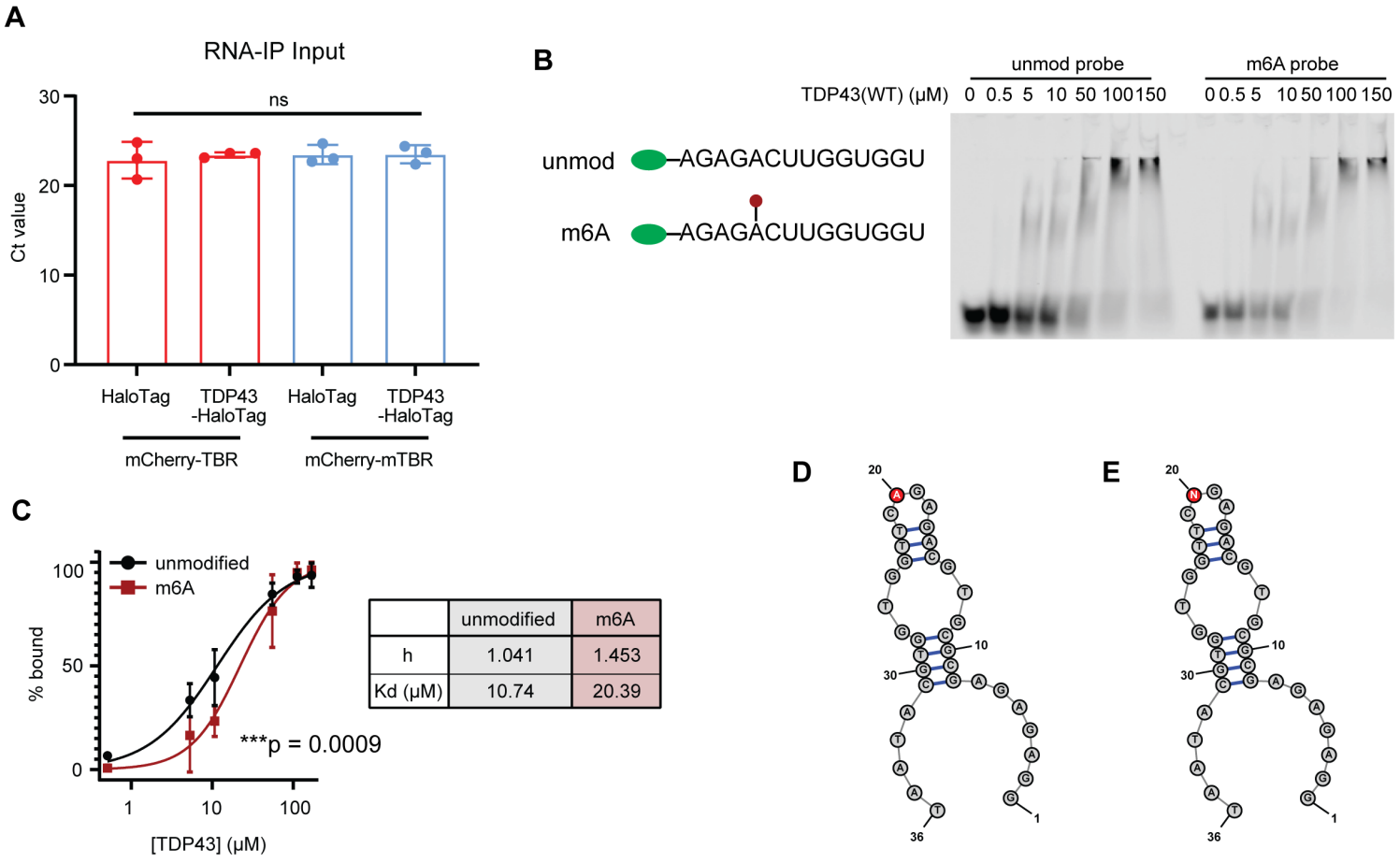

Supplemental figure 3: m6A modifications alter TDP43 binding capabilities (related to Fig. 3). (**A**) qRT-PCR cycle threshold (Ct) values from HaloTag-TDP43 HEK293T cells expressing mCherry-TBR or mCherry-mTBR. Data shown as mean ± SD. Individual points represent biological replicates. Ns, not significant by one-way ANOVA with Tukey's post-test. (**B**) Electromobility shift assay (EMSA) demonstrating binding of recombinant TDP43(WT) to 14nt probe modeled after the TDPBR, with and without m6A modification. Probe concentration was kept constant at 500 pM. (**C**) Percent bound m6A modified (red) or unmodified (black) RNA probe, plotted as nonlinear regression with Hill slope. ***$p < 0.0009$; extra-sum-of-squares F test. RNA secondary structure prediction for unmodified (**D**) and m6A-modified (**E**) CLIP34nt region of the *TARDBP* 3'UTR, using RNAstructure software. The methylated residue is red in each schematic.

Supplemental Figure 4: Intersection of TDP43 pathology and m6A modified substrates in ALS

A

cluster ID	#	examples	top KEGG pathway
1	14	TP53, CARM1, CSNK2A1, SP1, MAPK9	apoptosis
2	8	NUP214, NUP98, TNPO2, NDC1	RNA transport
3	6	WASF2, MYL6, CDC42, ARPC2	bacterial invasion
4	6	HNRNPC, NONO, PTBP1, SRSF10	spliceosome
5	4	ASXL1, RNF2, UBAP2L, MAPKAPK3	VEGF signaling

B

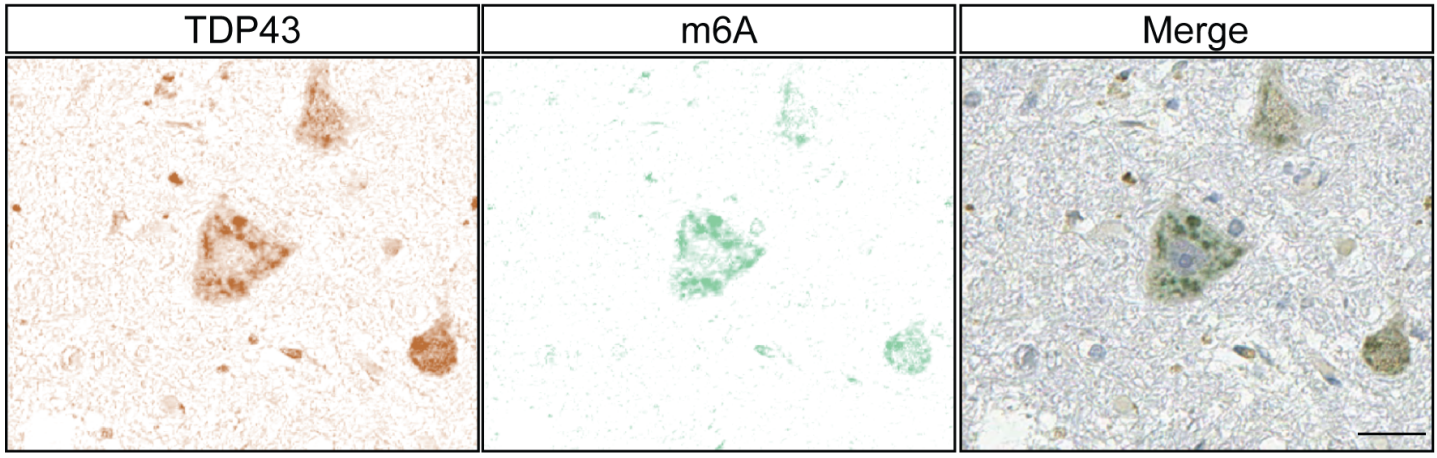

C

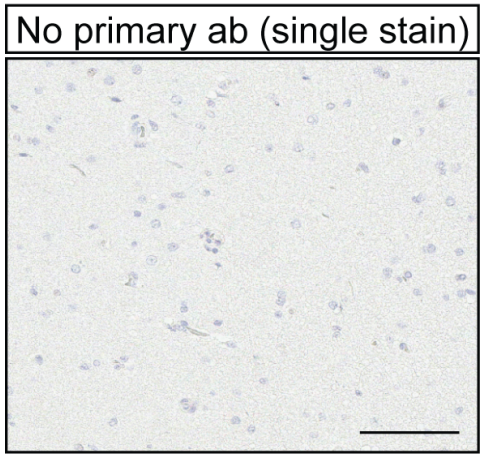

D

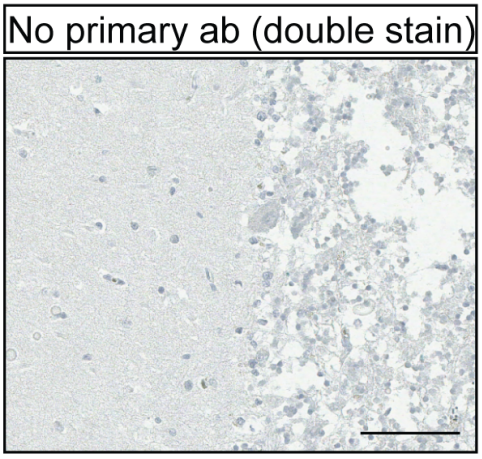

Supplemental figure 4: Intersection of TDP43 pathology and m6A modified substrates in ALS (related to Fig. 4). (**A**) Protein-protein interaction network analysis[2] for 322 hypermethylated TDP43 targets (A1, **Fig. 4G**), showing enrichment for proteins functioning in apoptosis, RNA transport, splicing, and VEGF signaling. (**B**) Two-color immunohistochemistry for TDP43 (brown) and m6A (green) in sALS spinal cord. The merged image includes a Hematoxylin counter stain for designation of the nucleus. Scale bar, 20μm. Controls include sections stained only with anti-mouse (**C**) or anti-mouse and anti-rabbit (**D**) secondary antibodies. Scale bar for (**C**) and (**D**), 100μm.

Supplemental Fig. 5: TDP43-mApple expression is proportional to intensity and toxicity

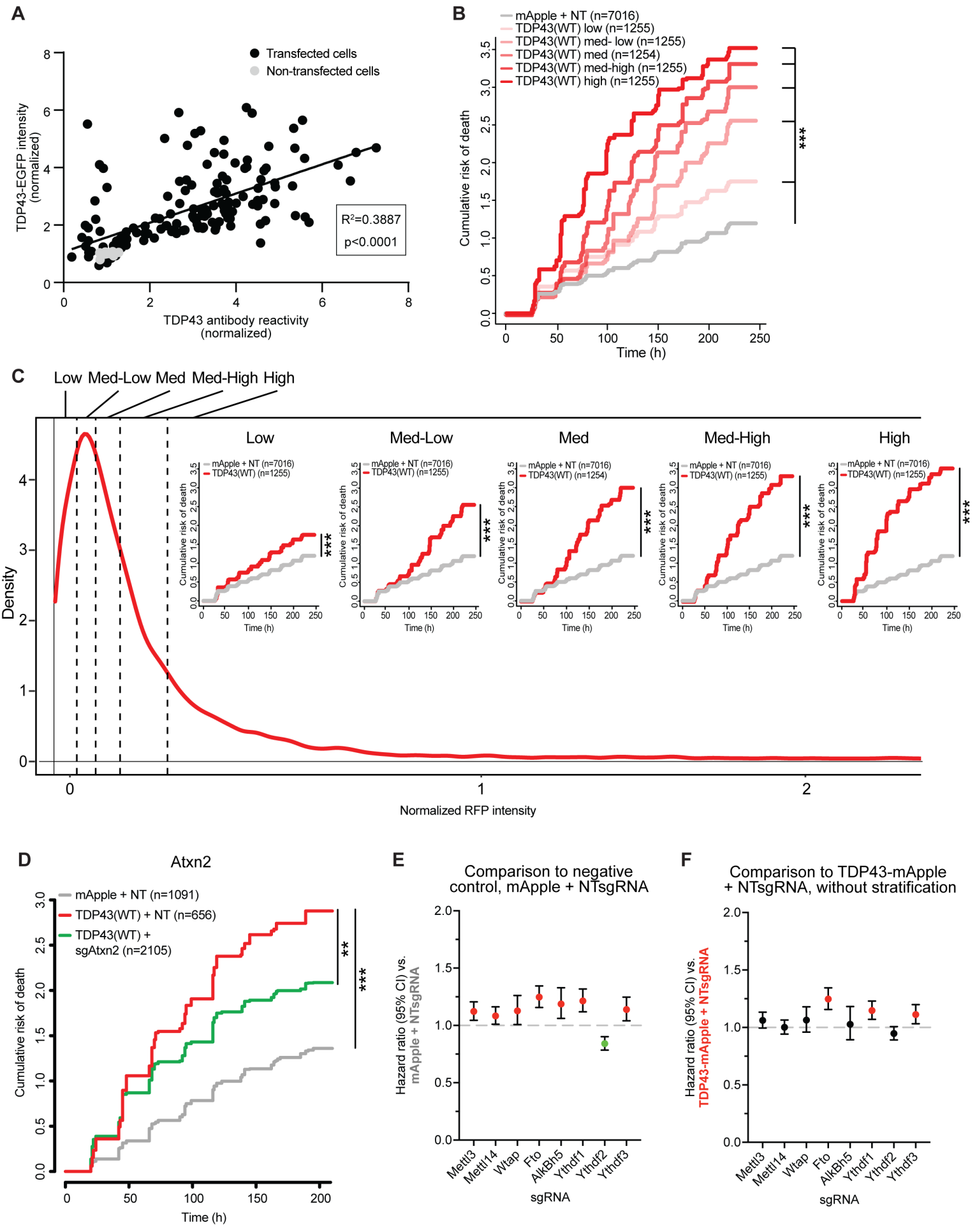

Supplemental figure 5: TDP43-mApple expression is proportional to intensity and toxicity (related to Fig. 5). (**A**) Correlation of single-cell TDP43 protein levels, determined by immunostaining, and RFP fluorescence in neurons overexpressing TDP43(WT)-mApple. Black: transfected cells, n= 144; grey: non-transfected cells, n= 20. (**B**) Neurons were stratified into 5 quintiles of equal cell number based on TDP43(WT)-mApple intensity, and their risk of death compared via Cox proportional hazards analysis. n= 7016 for mApple + NT; n= 1254 or 1255 cells per quintile. TDP43(WT)-mApple expression is significantly more toxic at all quintiles compared to mApple control: Low HR= 1.38, Med-Low HR= 1.85, Med HR= 2.18, Med-High HR= 2.47, High HR= 2.89. ***p $<2.0 \times 10^{-16}$ for all quintiles, Cox proportional hazards analysis. (**C**) Density plot of normalized RFP fluorescence illustrating separation of TDP43(WT)-mApple expression quintiles. Inset graphs correspond to neuronal survival in each quintile, same data as displayed in **B**. ***p $<2.0 \times 10^{-16}$ for all quintiles, Cox proportional hazards analysis. (**D**) Atxn2 knockout effectively reduces the risk of death in rodent primary neurons overexpressing TDP43 ***$p<2.0 \times 10^{-16}$, HR= 2.25; **$p=6.5 \times 10^{-4}$, HR= 0.85). (**E**) With the exception of *Ythdf2*, knockout of most m6a factors increased the risk of death in control rodent primary neurons expressing mApple and NT sgRNA. Plots show hazard ratio (HR) compared to mApple + NT sgRNA, $\pm$ 95% CI. Dotted line represents HR=1, the reference value for mApple + NT sgRNA. (**F**) Relative survival of neurons expressing TDP43-mApple upon knockout of m6A factors, in comparison to TDP43-mApple + NT sgRNA, without stratification for TDP43-mApple expression levels. Dotted line represents HR=1, the reference value for TDP43-mApple + NT sgRNA. For (C)-(F) statistical significance determined by Cox proportional hazards, with a minimum of 3 biological replicates per condition.

Supplemental Fig. 6: YTHDF2 in sALS patient samples and iPSC-derived neurons

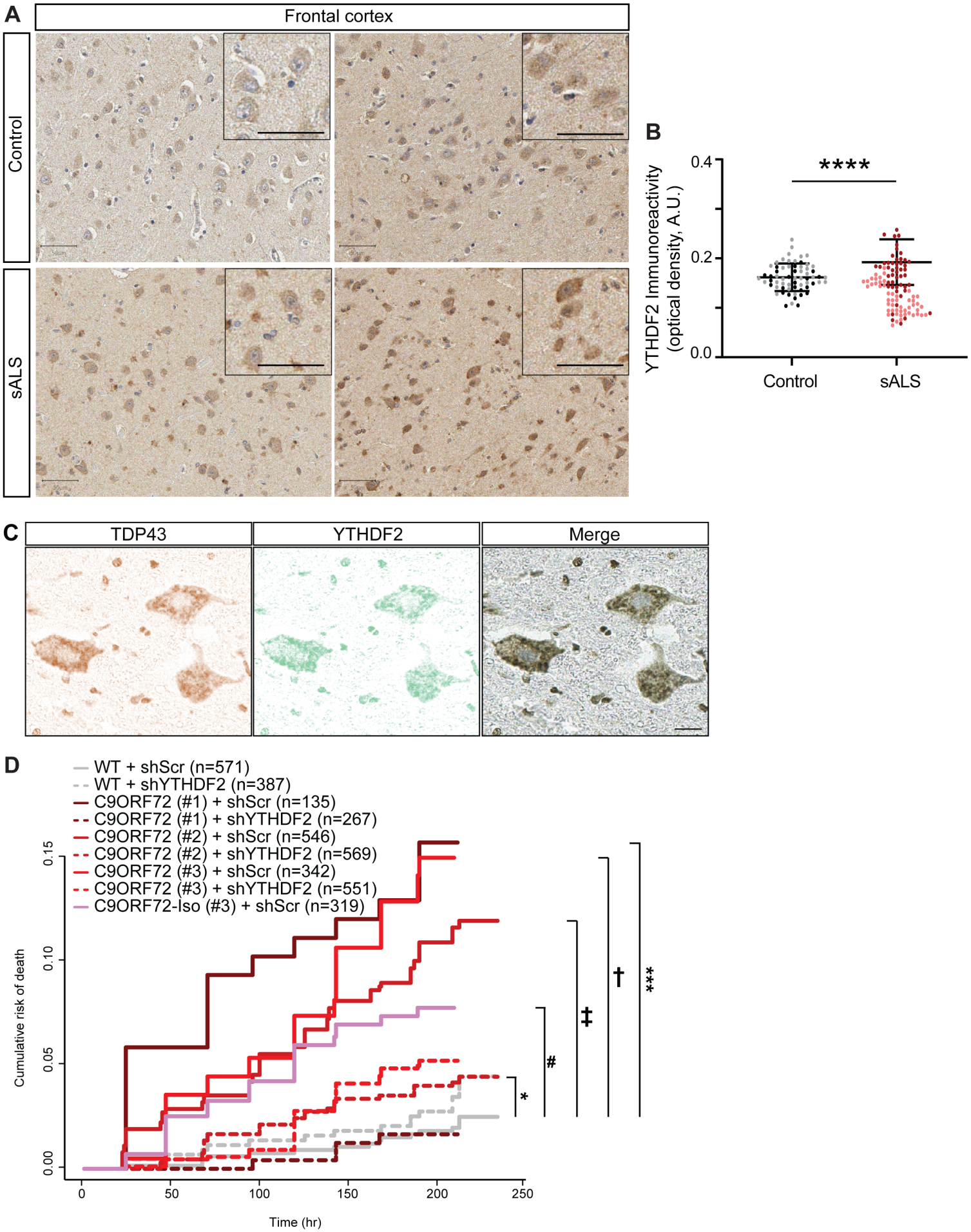

Supplemental figure 6: YTHDF2 in patient samples and iPSC-derived neurons (related to Fig. 6). (**A**) Immunostaining of YTHDF2 in control and sALS patient frontal cortex samples. Scale bar= 50μm. (**B**) Quantification of YTHDF2 immunoreactivity in frontal cortex neurons from control (n= 65) and sALS (n= 99) samples. ****p<0.0001, Mann-Whitney test. (**C**) Two-color immunohistochemistry of TDP43 (brown) and YTHDF2 (green) in sALS spinal cord. Hematoxylin counter stain outlines the nucleus in the merged image. Scale bar= 20μm. (**D**) Knockout of YTHDF2 in *C9ORF72* iNeurons reduces toxicity (***p = 1.33×10^{-6}, HR= 7.36; †p= 6.74×10^{-9}, HR= 5.21; ‡p= 1.16×10^{-3}, HR= 6.90; #p= 0.045, HR= 1.9. *p= 0.031, HR= 3.66). Statistical significance determined by Cox proportional hazards.

Table S1: Post-mortem samples (related to Figs. 4 and 6)

Diagnosis	Age	Sex	Experiment
Control 1	66	M	m6A array (Fig. 4)
Control 2	85	M	m6A array (Fig. 4)
Control 3	68	M	m6A array (Fig. 4)
sALS 1	65	M	m6A array (Fig. 4)
sALS 2	64	M	m6A array (Fig. 4)
sALS 3	65	M	m6A array (Fig. 4)
sALS 4	81	M	m6A array (Fig. 4)
Control 4	76	F	m6A IHC (Fig. 4)
Control 5	88	M	m6A IHC, YTHDF2 IHC (Figs. 4 and 6)
Control 6	56	M	m6A IHC, YTHDF2 IHC (Figs. 4 and 6)
ALS 1	66	F	m6A IHC (Fig. 4)
ALS 2	64	M	m6A IHC (Fig. 4)
ALS 3	68	M	m6A IHC (Fig. 4)
Control 7	48	M	YTHDF2 IHC (Fig. 6)
ALS 4	76	M	YTHDF2 IHC (Fig. 6)
ALS 4	60	F	YTHDF2 IHC (Fig. 6)
ALS 6	99	M	YTHDF2 IHC (Fig. 6)

Table S2: Plasmids (related to STAR Methods)

Construct	Reference/ Source	sgRNA target	sgRNA sequence (5' to 3')
pGW1-EGFP	refs.[4,5]	N/A	N/A
pGW1-mApple	refs.[4,5]	N/A	N/A
pGW1-TDP43(WT)-EGFP	refs.[4,5]	N/A	N/A
pGW1-Halo	ref.[6]	N/A	N/A
pGW1-TDP43-TEV-Halo	ref.[7]	N/A	N/A
pCMV-APOBEC1-YTH	ref.[8]	N/A	N/A
pCMV-APOBEC1-YTHmut	ref.[8]	N/A	N/A
pCaggs-mCherry-TBR	refs.[6,7,9]	N/A	N/A
pE-6xHis-SUMO-TDP43(WT)	ref.[7]	N/A	N/A
CFTR minigene	ref.[3]	N/A	N/A
pSpCas9(BB)-2A-GFP	Addgene #48138	N/A	N/A
pcDNA-flag-YTHDF2	Addgene #52300	N/A	N/A
pcDNA-flag-METTL3	Addgene #53739	N/A	N/A
pcDNA-flag-METTL14	Addgene #53740	N/A	N/A
GIPZ Non-silencing Lentiviral shRNA Control	Horizon Discovery #RHS4346	N/A	N/A
GIPZ Lentiviral Human YTHDF2 shRNA	Horizon Discovery #RHS4430-200182983	N/A	N/A

pGW1-YTHDF2-Halo	This paper	N/A	N/A
pGW1-YTHDF2-2A-GFP	This paper	N/A	N/A
pCaggs-mCherry-mTBR	This paper	TARDBP 3' UTR, SDM A-G	F: CATTATGCACCACCAAGCCTCTGCACGCGCTCTC
			R: GCTTTGCAGGAGGGCTTGAAGCAGAG
pSpCas9(BB)-2A-GFP + NeuN sgRNA	This paper	NeuN	F: CACCGACCGTCTGGGTCCCAGCGAT
			R: AAACATCGCTGGGACCCAGACGGTC
pSpCas9(BB)-2A-GFP + Mettl3 sgRNA	This paper	Mettl3	F: CACCGGCTGGGCTTAGGGCCACTAG
			R: AAACCTAGTGGCCCTAAGCCCAGCC
pSpCas9(BB)-2A-GFP + Mettl14 sgRNA	This paper	Mettl14	F: CACCGGATTCTTCTGGAGCCTCCTC
			R: AAACGAGGAGGCTCCAGAAGAATCC
pSpCas9(BB)-2A-GFP + Wtap sgRNA	This paper	Wtap	F: CACCGGCCGCCAGTCACACAGGCCG
			R: AAACCGGCCTGTGTGACTGGCGGCC
pSpCas9(BB)-2A-GFP + Fto sgRNA	This paper	Fto	F: CACCGGCTGCACAAAGAGGTCCCCG
			R: AAACCGGGGACCTCTTTGTGCAGCG
pSpCas9(BB)-2A-GFP + Alkbh5 sgRNA	This paper	Alkbh5	F: CACCGGCCTGCCTTGTAGTTGTCCC
			R: AAACGGGACAACTACAAGGCAGGCC
pSpCas9(BB)-2A-GFP + Ythdf1 sgRNA	This paper	Ythdf1	F: CACCGGCTGTTTTTGGGCAACCTGG
			R: AAACCCAGGTTGCCCAAAAACAGCC
pSpCas9(BB)-2A-GFP + Ythdf2 sgRNA	This paper	Ythdf2	F: CACCGGCTGTAGTAACTGGGTAAGT
			R: AAACACTTACCCAGTTACTACAGCC
pSpCas9(BB)-2A-GFP + Ythdf3 sgRNA	This paper	Ythdf3	F: CACCGGCTCTCCCAAGAGAACTAGG
			R: AAACCCTAGTTCTCTTGGGAGAGCC
pSpCas9(BB)-2A-GFP + Atxn2 sgRNA	This paper	Atxn2	F: CACCGCAGCAGTTCTCGAGGAGGG
			R: AAACCCCTCCTCGAGAACTGCTGC

Table S3: Antibodies (related to STAR Methods)

Target	Source	Catalog #	RRID	Species	Dilution
TDP43	Proteintech	10782-2-AP	AB_2892214	Rabbit	1:100
NeuN	Cell Signaling Technologies	24307T	AB_2651140	Rabbit	1:500
YTHDF2	Proteintech	24744-1-AP	AB_2687435	Rabbit	1:100
m6A	Millipore Sigma	ABE572	AB_2892213	Rabbit	1:500
m6A	Cell Signaling Technologies	56593S	AB_2799515	Rabbit	1:500
m6A	Millipore Sigma	ABE572-I-100UG	AB_2892214	Rabbit	1:500
HaloTag ligand (JF646 dye)	Promega	GA1120	N/A	N/A	1:20,000
Anti-rabbit Alexa Fluor 488 (secondary antibody)	ThermoFisher	A-11034	N/A	Goat	1:250
Anti-rabbit HRP (secondary antibody)	Jackson ImmunoResearch Labs Inc.	111-035-003	N/A	Goat	1:10,000

Table S4: Oligonucleotides (related to STAR Methods)

Target	Source	Sequence (5' to 3')
mCherry	This paper	F: ATGGTGAGCAAGGGCGAGGA
		R: GATCTCGAACTCGTGGCC
CFTR	Ayala *et al.*, 2006[3]	F: caacttcaagctcctaagccactgc
		R: taggatccggtcaccaggaagttggttaaatca
Clip34nt_unmodified	This paper	5IR800CWN-AGAGACUUGGUGGU
Clip34nt_m6A	This paper	5IR800CWN-AGAG/iN6Me-A/CUUGGUGGU
N_TARDBP_F	This paper	CACCGGAAATACCATCGGAAGACGA
N_TARDBP_R	This paper	CACCGGGGCTCATCGTTCTCATCTT
YTHDF2_F	This paper	GATGCCGCCTATCGTTCCAT
YTHDF2_R	This paper	ACGTCAAAACGACCCTTCCA
TARDBP_F	This paper	GTGGCTCTAATTCTGGTGCAG
TARDBP_R	This paper	CACAACCCCACTGTCTACATT
XIST_F	This paper	CCCTACTGCGCTTTTTGCTG
XIST_R	This paper	AAATGCAAGGGCGACTGGTA
MAPK14_F	This paper	GCATAATGGCCGAGCTGTTG
MAPK14_R	This paper	TGGCTTGGCATCCTGTTAATG
GAPDH_F	This paper	AAGGTGAAGGTCGGAGTCAA
GAPDH_R	This paper	AATGAAGGGGTCATTGATGG

Table S5: Cell lines (related to STAR Methods)

Name	Source	Identifier
HEK293T	ATCC	CRL-3216
Primary rat neurons	Charles River Laboratories	Long-Evans rats (Crl:LE)
Human iPSCs	University of Michigan ALS Repository	1021, 0883, 0312
	Cedars Sinai iPSC Repository	Cs29i, Cs29

Table S6: Human iPSC lines (related to STAR Methods)

Line	Identifier	Gene	Mutation	Sex	Age at biopsy	Age at onset	Tag	Integrated cassette
1021	WT	*TARDBP*	-	F	54	-	TDP43-Dendra 2 (C)	CLYBL:TO-hNgn1/2[6]
1021	M337V	*TARDBP*	Isogenic M337V[10]	F	54	-	TDP43-Dendra 2 (C)	CLYBL:TO-hNgn1/2[6]
312	C9ORF72 (#1)	*C9ORF72*	HRE	M	52	54	-	CLYBL:TO-hNgn1/2[6]
883	C9ORF72 (#2)	*C9ORF72*	HRE	M	49	51	-	CLYBL:TO-hNgn1/2[6]
Cs29i	C9ORF72 (#3)	*C9ORF72*	HRE	M	47	NA	-	CLYBL:TO-hNgn1/2[6]
Cs29i	C9ORF72 ISO (#3)	*C9ORF72*	Isogenic corrected[11]	M	47	NA	-	CLYBL:TO-hNgn1/2[6]

NA: not assessed; HRE, hexanucleotide repeat expansion mutation; (C), carboxyl terminus

Supplemental References

1. Hallegger, M., Chakrabarti, A.M., Lee, F.C.Y., Lee, B.L., Amalietti, A.G., Odeh, H.M., Copley, K.E., Rubien, J.D., Portz, B., Kuret, K., et al. (2021). TDP-43 condensation properties specify its RNA-binding and regulatory repertoire. Cell *184*, 4680-4696.e22. 10.1016/J.CELL.2021.07.018.

2. Szklarczyk, D., Gable, A.L., Nastou, K.C., Lyon, D., Kirsch, R., Pyysalo, S., Doncheva, N.T., Legeay, M., Fang, T., Bork, P., et al. (2021). The STRING database in 2021: customizable protein–protein networks, and functional characterization of user-uploaded gene/measurement sets. Nucleic Acids Res. *49*, D605. 10.1093/NAR/GKAA1074.

3. Ayala, Y.M., Pagani, F., and Baralle, F.E. (2006). TDP43 depletion rescues aberrant CFTR exon 9 skipping. FEBS Lett. *580*, 1339–1344. 10.1016/J.FEBSLET.2006.01.052.

4. Barmada, S.J., Skibinski, G., Korb, E., Rao, E.J., Wu, J.Y., and Finkbeiner, S. (2010). Cytoplasmic mislocalization of TDP-43 is toxic to neurons and enhanced by a mutation associated with familial amyotrophic lateral sclerosis. J. Neurosci. *30*, 639–649. 10.1523/JNEUROSCI.4988-09.2010.

5. Barmada, S.J., Serio, A., Arjun, A., Bilican, B., Daub, A., Ando, D.M., Tsvetkov, A., Pleiss, M., Li, X., Peisach, D., et al. (2014). Autophagy induction enhances TDP43 turnover and survival in neuronal ALS models. Nat. Chem. Biol. *10*, 677. 10.1038/NCHEMBIO.1563.

6. Weskamp, K., Tank, E.M., Miguez, R., McBride, J.P., Gómez, N.B., White, M., Lin, Z., Gonzalez, C.M., Serio, A., Sreedharan, J., et al. (2020). Shortened TDP43 isoforms upregulated by neuronal hyperactivity drive TDP43 pathology in ALS. J. Clin. Invest. *130*, 1139–1155. 10.1172/JCI130988.

7. Flores, B.N., Li, X., Malik, A.M., Martinez, J., Beg, A.A., and Barmada, S.J. (2019). An Intramolecular Salt Bridge Linking TDP43 RNA Binding, Protein Stability, and TDP43-Dependent Neurodegeneration. Cell Rep. *27*, 1133-1150.e8. 10.1016/j.celrep.2019.03.093.

8. Meyer, K.D. (2019). DART-seq: an antibody-free method for global m6A detection. Nat. Methods, 1–6. 10.1038/s41592-019-0570-0.

9. Barmada, S.J., Ju, S., Arjun, A., Batarse, A., Archbold, H.C., Peisach, D., Li, X., Zhang, Y., Tank, E.M.H., Qiu, H., et al. (2015). Amelioration of toxicity in neuronal models of amyotrophic lateral sclerosis by hUPF1. Proc. Natl. Acad. Sci. U. S. A. *112*, 7821–7826. 10.1073/PNAS.1509744112.

10. Sidibé, H., Khalfallah, Y., Xiao, S., Gómez, N.B., Fakim, H., Tank, E.M.H., Tomasso, G. Di, Bareke, E., Aulas, A., McKeever, P.M., et al. (2021). TDP-43 stabilizes G3BP1 mRNA: relevance to amyotrophic lateral sclerosis/frontotemporal dementia. Brain *144*, 3461. 10.1093/BRAIN/AWAB217.

11. Ho, R., Workman, M.J., Mathkar, P., Wu, K., Kim, K.J., O'Rourke, J.G., Kellogg, M., Montel, V., Banuelos, M.G., Arogundade, O.A., et al. (2021). Cross-Comparison of Human iPSC Motor Neuron Models of Familial and Sporadic ALS Reveals Early and Convergent Transcriptomic Disease Signatures. Cell Syst. *12*, 159-175.e9. 10.1016/J.CELS.2020.10.010.

12. Kierzek, E., Zhang, X., Watson, R.M., Kennedy, S.D., Szabat, M., Kierzek, R., and

Mathews, D.H. (2022). Secondary structure prediction for RNA sequences including N6-methyladenosine. Nat. Commun. 2022 131 *13*, 1–10. 10.1038/s41467-022-28817-4.